Environmental Engineering Research

Environ. Eng. Res. 2014 March,19(1) : 15-22

Research Paper

http://dx.doi.org/10.4491/eer.2014.19.1.015
pISSN 1226-1025 eISSN 2005-968X

Adsorption Characteristics of Multi-Metal Ions by Red Mud, Zeolite, Limestone, and Oyster Shell

Woo-Seok Shin[1], Ku Kang[1], Young-Kee Kim[1,2†]

[1]*Institute of Marine Science and Technology Research, Hankyong National University, Anseong 456-749, Korea*
[2]*Department of Chemical Engineering and Research Center of Chemical Technology, Hankyong National University, Anseong 456-749, Korea*

Abstract

In this study, the performances of various adsorbents—red mud, zeolite, limestone, and oyster shell—were investigated for the adsorption of multi-metal ions (Cr^{3+}, Ni^{2+}, Cu^{2+}, Zn^{2+}, As^{3+}, Cd^{2+}, and Pb^{2+}) from aqueous solutions. The result of scanning electron microscopy analyses indicated that the some metal ions were adsorbed onto the surface of the media. Moreover, Fourier transform infrared spectroscopy analysis showed that the Si(Al)-O bond (red mud and zeolite) and C-O bond (limestone and oyster shell) might be involved in heavy metal adsorption. The changes in the pH of the aqueous solutions upon applying adsorbents were investigated and the adsorption kinetics of the metal ions on different adsorbents were simulated by pseudo-first-order and pseudo-second-order models. The sorption process was relatively fast and equilibrium was reached after about 60 min of contact (except for As^{3+}). From the maximum capacity of the adsorption kinetic model, the removal of Pb^{2+} and Cu^{2+} were higher than for the other metal ions. Meanwhile, the reaction rate constants ($k_{1,2}$) indicated the slowest sorption in As^{3+}. The adsorption mechanisms of heavy metal ions were not only surface adsorption and ion exchange, but also surface precipitation. Based on the metal ions' adsorption efficiencies, red mud was found to be the most efficient of all the tested adsorbents. In addition, impurities in seawater did not lead to a significant decrease in the adsorption performance. It is concluded that red mud is a more economic high-performance alternative than the other tested adsorption materials for applying a removal of multi-metal in seawater.

Keywords: Adsorption, Lime stone, Multi-metals, Red mud, Seawater, Zeolite

1. Introduction

Sediments contaminated by heavy metals cause a worldwide environmental pollution problem. Heavy metals accumulated in sediments have adverse effects on benthic organisms. The metals also elute into seawater and affect the marine ecosystem, the health of residents and tourists in coastal regions, and the safety of fish products obtained from the shore [1]. Therefore, several techniques have been studied and developed to remediate heavy-metal-contaminated marine sediments [2].

As ocean disposal of contaminated sediment is not acceptable, the options for remediation are *in situ* capping, *in situ* treatment, removal and containment, and removal and treatment. From an economic perspective, treatment for reducing the contamination (e.g., extraction, ion exchange, etc.) is not a favorable option. *In situ* capping and containment in sub-aqueous pits are considered as the more economical alternatives [3]. These methods essentially require capping materials that should be able to isolate and/or stabilize the contaminants from the benthic environment, prevent contaminated sediment resuspension, and reduce the contaminant flux to the benthic water. They should also be cheap and easily obtainable. Sand, gravel, and stone armor have conventionally been used as capping materials, but they can only provide physical isolation and the prevention of resuspension. Therefore, reactive capping materials have recently been spotlighted as an alternative serving not only to physically isolate and prevent resuspension, but also to stabilize and reduce the flux of the dissolved contaminants.

Previous studies have shown that the capping of clean sediment amendments and *in situ* chemical immobilization reduce the mobility and bioavailability of heavy metals through either adsorption or precipitation [4, 5]. It has also been reported that some materials, such as lime and zeolites, are useful for chemical immobilization of heavy metals in degraded soils [6, 7].

In this work, red mud, natural zeolite, natural limestone, and crushed oyster shell were examined as capping materials. Red mud is a solid waste residue formed after the caustic digestion of bauxite ores during the production of alumina. For every tonne

This is an Open Access article distributed under the terms of the Creative Commons Attribution Non-Commercial License (http://creativecommons.org/licenses/by-nc/3.0/) which permits unrestricted non-commercial use, distribution, and reproduction in any medium, provided the original work is properly cited.

Received May 16, 2013 **Accepted** September 25, 2013

†Corresponding Author
E-mail: kim@hknu.ac.kr
Tel: +82-31-670-5206 Fax: +82-31-670-5209

of alumina produced, approximately one to two tonnes (dry weight) of bauxite residues are generated. Red mud, which is a cheap industrial by-product, is principally composed of oxides (e.g., silica, aluminum, iron, calcium, and titanium oxides) and hydroxides responsible for its good surface reactivity [8-10]. This adsorbent could be used to precipitate soluble metals in their insoluble hydroxide form in an alkaline environment [11]. Meanwhile, other researchers have previously reported the heavy metal removal characteristics of wastewater, mine drainage, and soil environments using red mud, zeolite, limestone, and oyster shell [12-15]. Moreover, these studies produced removal results of contamination with a single (or several) heavy metal(s) in a land environment system. However, contaminated seawater/or sediment commonly contains multiple heavy metal ions. Moreover, insufficient data exist that investigate the importance of multi-heavy metal adsorption mechanisms for *in situ* capping in marine contaminated sediments. Hence, it is necessary to research the adsorption characteristics in multi-heavy metal contaminated seawater (or sediment).

In this study, the adsorption characteristics of various adsorbents (red mud, natural zeolite, natural limestone, and oyster shell) were investigated using a solution spiked with multiple heavy metals (Pb^{2+}, Ni^{2+}, Cr^{3+}, Cd^{2+}, Cu^{2+}, Zn^{2+}, and As^{3+}). This work contributes to the understanding of the principal metal ion-sorbent interaction mechanisms and establishing of capping materials for the remediation of heavy metals in contaminated sediments.

2. Materials and Methods

2.1. Materials

The red mud (KC Co. Ltd., Yeongam, Korea), zeolite (Zeo-Soil; Rex Material Co. Ltd., Pohang, Korea), limestone, and oyster shell used for the experiments were of commercially available grade and provided by a domestic supplier. The original adsorbents were washed with distilled water and dried in an oven at 105°C ± 5°C for 24 hr, after which they were ground in a mortar and passed through woven wire meshed sieves (No. 35, followed by No. 10) to obtain adsorbents with diameters of 1.0–2.0 mm (except red mud, which particles were of size ≤0.25 mm). Chemical compositions of the particulate adsorbents were characterized by X-ray fluorescence (XRF) spectrometry (XRF-1700; Shimadzu Co., Kyoto, Japan). The XRF results revealed that red mud and natural zeolite were mainly composed of metal oxides, such as SiO_2, Al_2O_3, and Fe_2O_3. Meanwhile, chemical analysis results for limestone and oyster shell showed that these were mainly composed of CaO (94.9% and 90.9%, respectively) and small amounts of other components (Table 1). The surface areas were measured with the nitrogen adsorption method at the liquid nitrogen temperature (i.e., -196°C) using an Autosorb-iQ-Kr/MP surface area analyzer (Quantachrome Instruments, Boynton Beach, FL, USA). Four data points were used to construct the plot to derive the monolayer adsorption capacity with relative pressures between 0.05 and 0.3. The observations were interpreted following the Brunauer-Emmett-Teller (BET) method. The surface area was determined for adsorbents using the BET surface area analyzer. The functional groups of adsorbents were analyzed by Fourier transform infrared (FTIR) spectroscopy (VERTEX 70; Bruker, Ettlingen, Germany). The surface morphologies of the adsorbents were also observed by scanning electron microscopy (SEM; S-3500N; Hitachi Co., Tokyo, Japan).

2.2. Batch Adsorption Experiments

Stock solutions of Pb^{2+}, Ni^{2+}, Cr^{3+}, Cd^{2+}, Cu^{2+}, Zn^{2+}, and As^{3+} (1,000 mg/L) were prepared by dissolving $Ni(NO_3)_2{\cdot}6H_2O$, As_2O_3, $Cd(NO_3)_2{\cdot}4H_2O$, CrO_3, $Cu(NO_3)_2{\cdot}3H_2O$, $Pb(NO_3)_2$, and $Zn(NO_3)_2{\cdot}6H_2O$ in deionized water, respectively. All chemicals used were reagent grade and were obtained from Junsei Chemical Co., Ltd. (Tokyo, Japan) and Samchun Chemical Company (Pyongtaek, Korea). The experiment was performed in a 50-mL flask with continuous stirring of 100 rpm at a temperature of 25°C ± 0.5°C. The adsorbents (0.5 g) were added to 30 mL of the mixed metal aqueous solution containing 50 mg/L of each metal ion. Before the experiment, the initial pH of aqueous solutions was adjusted to pH 7 by adding 1 M HNO_3 and 1 M NaOH solutions. To investigate the effect of contact time, experiments were separately conducted for 10, 30, 60, 120, 180, 360, and 720 min.

The effect of seawater salts on the removal of metal ions was investigated. The seawater used for preparing the sample solution was collected from the Daecheon beach in Korea and filtered with a quantitative filter paper (pore size 3 μm, No. 6; Advantec MFS Inc., Dublin, CA, USA) to remove inert particles. The adsorbents (0.5 g) were put into a 50-mL plastic tube with 30 mL seawater containing multi-heavy metal at each metal concentration of 50 mg/L, and the sample tube was agitated at a constant temperature of 25°C ± 0.5°C for 360 min. A sample with the same concentration prepared with deionized water was used as a control.

The supernatants of all samples were filtered with PTFE syringe filters (pore size 0.45 μm; Puradisc 25; Whatman, Maidstone, Kent, UK) and the filtrates were analyzed by inductively coupled plasma mass spectrometry to measure the heavy metal concentrations. The filtrates were acidified with 2% HNO_3 to decrease the pH value below 3 to prevent precipitation before the measurement.

2.3. Data Analysis

The adsorption efficiency of heavy metal was calculated by the following equation:

Table 1. Physical and chemical properties of adsorbents (wt%)

Composition	SiO_2	Al_2O_3	TiO_2	Fe_2O_3	MgO	CaO	Na_2O	Surface area (m^2/g)
Red mud	20.1	28.4	6.6	27.6	ND	3.3	13.0	26.0
Zeolite	76.5	12.0	0.33	1.7	1.3	1.9	2.5	60.0
Limestone	3.0	1.3	0.1	0.3	ND	94.9	ND	0.08
Oyster shell	1.8	0.6	ND	0.3	1.2	90.9	2.2	0.60

ND: not detected.

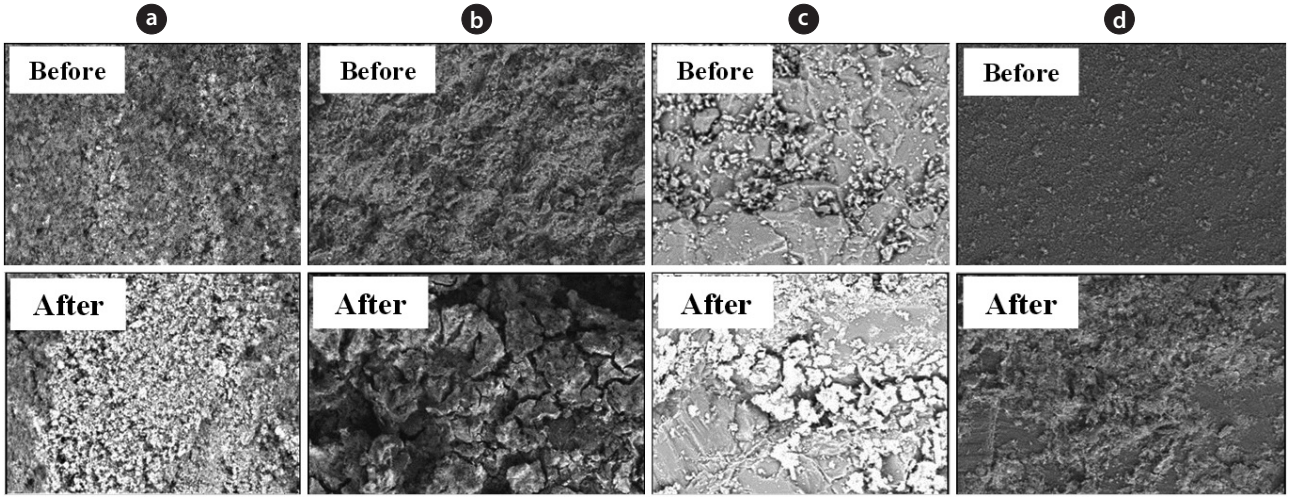

Fig. 1. Scanning electron microscopy images of the adsorbents before and after metal ion adsorption: (a) red mud (×1500), (b) zeolite (×500), (c) limestone (×1500), and (d) oyster shell (×500).

$$\text{Adsorption efficiency}\ (\%) = \frac{C_o - C}{C_o} \times 100, \quad (1)$$

where C_0 and C are the initial and final concentrations of a heavy metal (mg/L) in the sample solution, respectively.

To define the adsorption kinetics of heavy metal ions, the kinetic parameters were determined for contact times varying from 10 to 720 min. A pseudo-first-order equation, Eq. (2), and pseudo-second-order equation, Eq. (3), were used to fit the experimental data [16, 17]:

$$q_t = q_e\left[1-\exp\left(-k_1 t\right)\right], \quad (2)$$

$$q_t = \frac{t}{\frac{1}{k_2 q_e^2} + \frac{t}{q_e}}, \quad (3)$$

where q_t and q_e are the masses of adsorbed heavy metal per mass of adsorbent (mg/g) at a time t (min) and at equilibrium, respectively, and k_1 (min^{-1}) and k_2 (g mg^{-1} min^{-1}) are the rate constants of the pseudo-first-order and pseudo-second-order equations, respectively.

3. Results and Discussion

3.1. Characteristics of Adsorbents

SEM analyses were conducted to observe any changes in the surface structure of adsorbents before and after the sorption experiments. Analyses of the SEM images of the adsorbents after the metal ion experiments have shown that some metal ions were adsorbed onto the surface of the media. This result indicates the presence of an adsorption process (Fig. 1). These findings also show that the adsorption of metal ions onto the surfaces of adsorbents is likely due to the ion exchange/complexation reaction. Moreover, according to the result of XRF analysis (Table 1), the main chemical components of red mud were silica, alumina, and iron oxide; and its surface area is larger than those of limestone and oyster shell. This makes the red mud suitable for adsorbent [18].

The FTIR spectra of adsorbents, after heavy metal adsorption in the range of 500–4,000 cm^{-1}, are shown in Fig. 2. In the spectra of the red mud and zeolite, a band was present in the hydroxyl stretching region at 3,400–3,300 cm^{-1} in Fig. 2(a) and (b). This was likely due to the presence of H_2O in the red mud and zeolite [19, 20]. Besides, in the red mud and zeolite samples, a band was detected at 1,640 cm^{-1}. This was attributed to the water molecules occluded inside the alumino-silicate structure [20]. The band at 990–1,050 cm^{-1}, present in the red mud and zeolite samples, could be assigned to the stretching vibrations of Si(Al)-O. This band is sensitive to the content of structural Si and Al [5]. On the other hand, the intensities of the C-O bands of oyster shell and limestone between 1,400 and 500 cm^{-1} were the strongest [21]. We observed C-O stretching vibrations at 1,440–1,450 cm^{-1} and out-of-plane C-O bending vibrations at 870–880 cm^{-1}.

3.2. pH change of Solution by Adsorbents

Fig. 3 shows the pH change of the solution through the adsorption experiments by adding red mud, zeolite, limestone, and oyster shell for 720 min. The pH of the aqueous solution increased rapidly within 25 min when red mud was used, while the pH of the solution increased slightly from 7.00 to 7.16, 7.21, and 7.31 when zeolite, limestone, and oyster shell were applied, respectively in Fig. 3(a). During the alumina refining processes, a lot of base is added to the bauxite. Therefore, the red mud residues are strongly alkaline despite the washing during the process, and the pH of red mud has been reported to vary from 10 to 13 [22]. This is why red mud increased the pH of solution in our experiments. The OH^- ions not only cause an increase in the pH of the solution, but they also react with the metal ions to form precipitates [23]. Meanwhile, zeolite, limestone, and oyster shell cause small increases of pH compared to red mud, because these adsorbents are mainly composed of SiO_2 or CaO [24, 25]. On the other hand, the pH changes of the seawater solution from

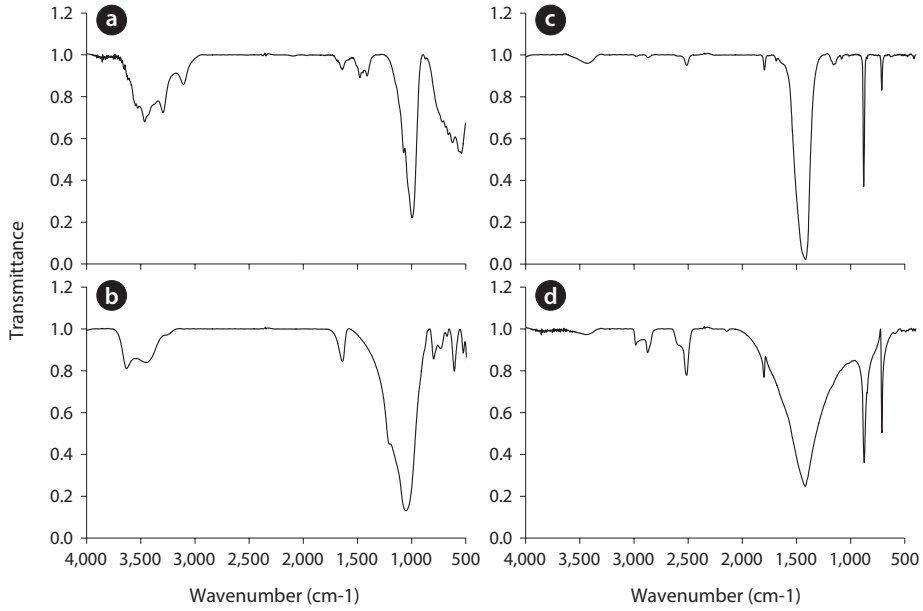

Fig. 2. Fourier transform infrared spectra of adsorbents after heavy metal adsorption: (a) red mud, (b) zeolite, (c) limestone, and (d) oyster shell.

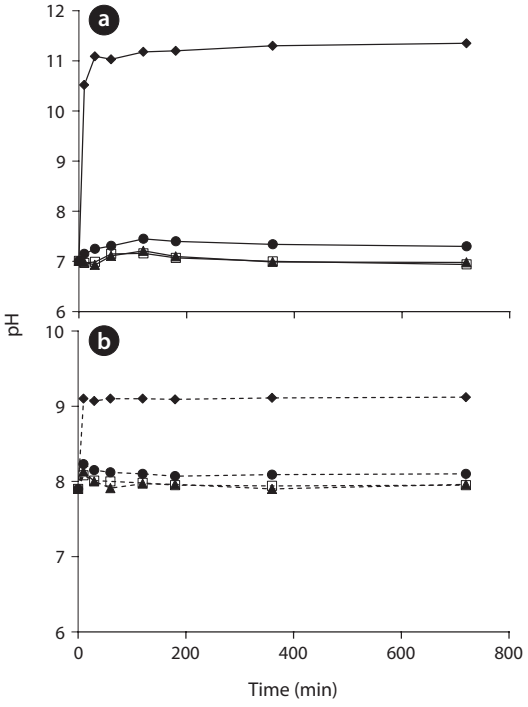

Fig. 3. The pH change of solution by adsorbents: (a) fresh water and (b) seawater. ♦: Red mud, □: zeolite, ▲: limestone, ●: oyster shell.

adding adsorbents were low compared to that of the fresh water solution in Fig. 3(b). This effect is due to the buffer ions in seawater impeding the increase of pH. From these results, the removal mechanisms of heavy metal ions by red mud might be not only surface adsorption and ion exchange, but also surface precipitation. It was also supported that the removal efficiency of some heavy metals, such as Ni, Zn, As, and Cd, in seawater solution (around pH 8) is higher than those in fresh water solution (around pH 7). However, the removal efficiencies of red mud in fresh water (around pH 11) and seawater (around pH 9) experiments were not significantly different, and the removal efficiency of red mud in seawater experiment (around pH 9) is much higher than those of other adsorbents in freshwater experiments (around pH 8). The high heavy metals adsorption capability of red mud can be explained by these results and by previous studies by other researchers [26, 27].

3.3. Adsorption Kinetics

Fig. 4 shows the adsorption kinetics of mixed metal ions solution by red mud, zeolite, limestone, and oyster shell. The curves of Cr^{3+}, Ni^{2+}, Pb^{2+}, Cu^{2+}, Cd^{2+}, and Zn^{2+} show that the adsorption rapidly reached equilibrium within 60 min; while the adsorption of As^{3+} ions was relatively slow in all experiments and it did not reach equilibrium within 720 min in the cases of zeolite and limestone. The kinetics parameters were calculated from eight data (means of at least three replicates) in each experiment and are summarized in Table 2. For red mud, the pseudo-first-order model fitted the data well for the Ni^{2+}, Cu^{2+}, Cd^{2+}, and Pb^{2+} ions and the pseudo-second-order model fitted the data well for the Cr^{3+}, Zn^{2+}, and As^{3+} ions. In the cases of zeolite, limestone, and oyster shell, the pseudo-first-order model could fit the data well for all metal ions. The pseudo-first-order equation showed good approximation to fit the experimental data (except for the Cr^{3+}, Zn^{2+}, and As^{3+} of red mud). The experimental q_e values were in agreement with the calculated values. Panayotova and Velikov [28, 29] investigated the removal kinetics of heavy metal ions (cadmium, lead, copper, nickel, and zinc) by natural zeolite and reported that the first-order kinetics showed good fitting to the data.

The calculated metal adsorption concentrations at equilibrium, listed in order of decreasing magnitude, are: Ni^{2+}, Cd^{2+}, Pb^{2+},

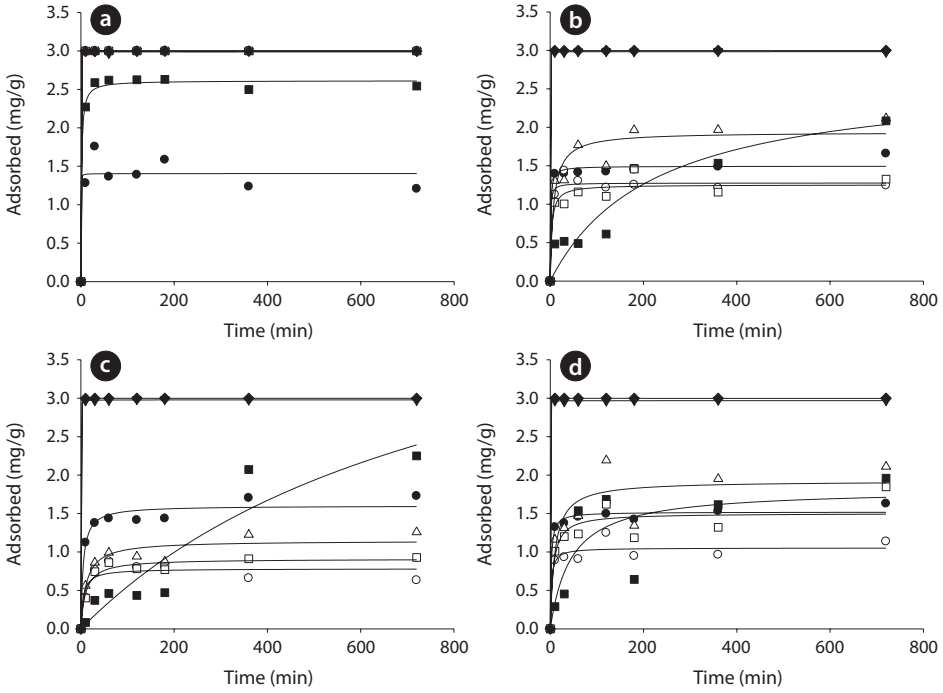

Fig. 4. Comparison of the measured and modeled adsorption time profiles for mixed heavy metal ions at pH 7: (a) red mud, (b) zeolite, (c) limestone, and (d) oyster shell. ●: Cr, ○: Ni, ▼: Cu, △: Zn, ■: As, □: Cd, ♦: Pb, solid line: pseudo-first-order model, dashed line: pseudo-second-order model.

Table 2. Kinetic model parameters of pseudo-first-order and pseudo-second-order equations and experimental results

Adsorbent	Metal ion	Experiments $q_{e,\,exp}$ (mg/g)	Model simulation		
			$q_{e,\,cal}$ (mg/g)	k_1 (min^{-1}) or k_2 (g/mg/min)	R^2
Red mud	$Cr^{3+,\,b}$	1.3644	1.4051	9.9537	0.8771
	$Ni^{2+,\,a}$	2.9990	2.9991	32,160.7	1.0000
	$Cu^{2+,\,a}$	2.9704	2.9906	137.01	0.9999
	$Zn^{2+,\,b}$	2.9935	2.9913	72.675	1.0000
	$As^{3+,\,b}$	2.6205	2.6133	0.2989	0.9946
	$Cd^{2+,\,a}$	2.9998	2.9986	5.9881	1.0000
	$Pb^{2+,\,a}$	2.9995	2.9934	17.367	0.9999
Zeolite	$Cr^{3+,\,b}$	1.4142	1.4725	0.2937	0.9758
	$Ni^{2+,\,a}$	1.3026	1.2767	0.2175	0.9745
	$Cu^{2+,\,a}$	2.9843	2.9824	0.6308	1.0000
	$Zn^{2+,\,a}$	1.7688	1.8082	0.0987	0.8648
	$As^{3+,\,a}$	0.4811	2.0792	0.0048	0.8858
	$Cd^{2+,\,a}$	1.1592	1.2035	0.1815	0.9036
	$Pb^{2+,\,a}$	2.9986	2.9976	6,717.40	1.0000
Limestone	$Cr^{3+,\,a}$	1.4361	1.6012	0.1299	0.9675
	$Ni^{2+,\,a}$	0.8790	0.7635	0.0883	0.9138
	$Cu^{2+,\,a}$	2.9734	2.9766	0.5847	1.0000
	$Zn^{2+,\,a}$	0.9909	1.0589	0.0657	0.8940
	$As^{3+,\,a}$	0.4611	3.1747	0.0019	0.8961
	$Cd^{2+,\,a}$	0.8619	0.8540	0.0658	0.9690
	$Pb^{2+,\,a}$	2.9981	2.9984	4.8963	1.0000
Oyster shell	$Cr^{3+,\,a}$	1.4577	1.4859	0.2185	0.9795
	$Ni^{2+,\,a}$	0.9075	1.0367	0.1914	0.9141
	$Cu^{2+,\,a}$	2.9606	2.9667	2,188.10	1.0000
	$Zn^{2+,\,a}$	1.4703	1.7957	0.0711	0.7946
	$As^{3+,\,a}$	1.5366	1.5331	0.0235	0.6870
	$Cd^{2+,\,a}$	1.2348	1.4177	0.1109	0.8307
	$Pb^{2+,\,a}$	2.9983	2.9983	6.9821	1.0000

[a]Values were determined by pseudo-first-order kinetic model. [b]Values were determined by pseudo-second-order kinetic model.

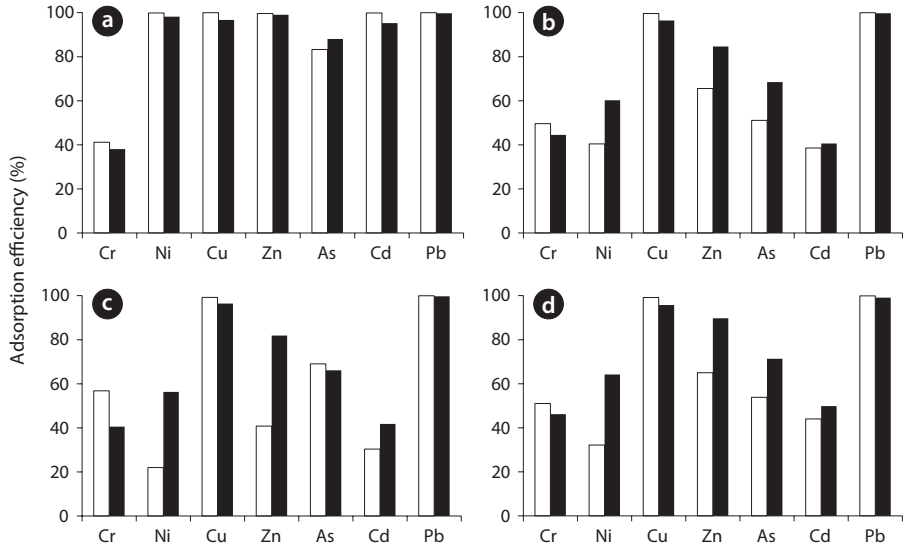

Fig. 5. Comparison of the adsorption performance in fresh water and seawater: (a) red mud, (b) zeolite, (c) limestone, and (d) oyster shell. White and black bars represent the results in fresh water and seawater, respectively.

Zn^{2+}, $Cu^{2+} > As^{3+} > Cr^{3+}$ for red mud; Pb^{2+}, $Cu^{2+} > As^{3+} > Zn^{2+} > Cr^{3+} > Ni^{2+}$, Cd^{3+} for zeolite; $As^{3+} > Pb^{2+}$, $Cu^{2+} > Cr^{3+} > Zn^{2+} > Cd^{2+} > Ni^{2+}$ for limestone; and Pb^{2+}, $Cu^{2+} > Zn^{2+} > As^{3+} > Cr^{3+} > Cd^{2+} > Ni^{2+}$ for oyster shell. Based on the maximum adsorption capacity of the kinetic model, the removal of Pb^{2+} and Cu^{2+} were higher than for the other metal ions. In general, the precipitations of soluble Pb and Cu as $Pb(OH)_2$ and $Cu(OH)_2$, are expected at pH values above 6 and 7, respectively [30]. Moreover, the affinity constants ($k_{1,2}$) are listed in order of decreasing magnitude: $Ni^{2+} > Cu^{2+} > Zn^{2+} > Pb^{2+} > Cr^{3+} > Cd^{2+} > As^{3+}$ for red mud; $Pb^{2+} > Cu^{2+} > Cr^{3+} > Ni^{2+} > Cd^{3+} > Zn^{2+} > As^{3+}$ for zeolite; $Pb^{2+} > Cu^{2+} > Cr^{3+} > Ni^{2+} \cong Cd^{3+} \cong Zn^{2+} > As^{3+}$ for limestone; and $Cu^{2+} > Pb^{2+} > Cr^{3+} > Ni^{2+} > Cd^{3+} > Zn^{2+} > As^{3+}$ for oyster shell. Based on the $k_{1,2}$ value of the model, the adsorption rate of As^{3+} was slower than for the other metal ions. In general, the predominant species of arsenic are H_3AsO_3 and $H_2AsO_3^-$ in the aqueous phase, in the pH range of 7.0–11.0 [30]. As the pH increases, the amount of negative arsenic species increases, while the positively charged surface sites decrease, up to the pH_{zpc} [31]. The experimental values ($q_{e,exp}$) of the mass of adsorbed metal ions per mass of adsorbent at equilibrium are in agreement with the calculated values as listed in Table 2. This supports that the rate-limiting step of the adsorption system is not the mass transfer in the solution, but the chemical and/or physical adsorption [32, 33]. The reaction rate constants (k_1) for zeolite, limestone, and oyster shell are low (0.0019–6.9821 min^{-1}) except for Pb^{2+} on zeolite (6,717.4 min^{-1}) and Cu^{2+} on oyster shell (2,188.1 min^{-1}). Meanwhile, red mud showed higher adsorption rate constants (9.9537–32,160.67) k_1 (min^{-1}) or k_2 (g mg^{-1} min^{-1}) with the exception of As^{3+} and Cd^{2+} than the other adsorbents. For instance, the surface areas of zeolite, red mud, oyster shell, and limestone have been reported as 60.0, 26.0, 0.6, and 0.08 m^2/g, respectively (Table 1). These surface area results are in agreement with the results obtained by other studies [11, 13, 34, 35]. It is proposed that physical adsorption plays little role in the interaction between the adsorbent and the heavy metal ions, because the adsorbents used for the experiments have small surface areas.

3.4. Comparison of Adsorption Efficiencies in Fresh Water and Seawater

Adsorption efficiencies of metal ions in fresh water and seawater were compared and the results are shown in Fig. 5. The adsorption efficiency of metal ions (except for Cr^{3+}) on red mud was the highest compared with those of other adsorbents, regardless of the type of water. Moreover, the adsorption efficiency of metal ions was higher in fresh water than seawater (except for As^{3+}). According to Hatje et al. [36], both the rate and extent of adsorption were reduced in seawater compared to freshwater. The reason is probably the competition between metals and major seawater cations (particularly Ca^{2+} and Mg^{2+}) for active sites on the particles and for chlorocomplexation [36]. At pH higher than 7, however, the results on zeolite, limestone, and oyster shell show that the adsorption efficiencies of several metals (e.g., Ni^{2+}, Cd^{3+}, Zn^{2+}, and As^{3+}) in seawater are higher than in fresh water. In particular, the effect of the increased ionic strength in seawater was more important for Ni^{2+} and Zn^{2+} than for the other metal ions. It has been suggested that double-charged surface species are responsible for promoting sorption at high ionic strength; when surface coverage is decreased, the electrostatic repulsion decreases and the promotive ionic effect disappears [37]. Hence, it can be concluded that the occurrence of promotive ionic strength effects may depend on the experimental conditions chosen. The mobility of metal ions in between seawater and fresh water depends on several factors including pH and ion composition [37]. Therefore, the adsorption behaviors of the examined metals varied according to pH conditions. These results have important implications on the comportment of trace metals in marine contaminated sediment. In particular, the adsorbents of red mud could be successfully used to adsorb heavy metals from marine contaminated sediments.

4. Conclusions

In this study, the adsorption characteristics of heavy metals on red mud, zeolite, limestone, and oyster shell were investigated. Results showed that the removal of heavy metal ions by the adsorbents was dependent on the system employed (e.g., adsorbent dose, temperature, and contact time) and was mainly dependent on the initial pH of the solution. The adsorption kinetics of all metal ions on zeolite (except for Cr^{3+}), limestone, and oyster shell was fitted using a pseudo-first-order equation. The results on red mud showed that the pseudo-first-order model fitted the data well for Ni^{2+}, Cu^{2+}, Cd^{2+}, and Pb^{2+} ions, and the pseudo-second-order model fitted the data well for Cr^{3+}, Zn^{2+}, and As^{2+} ions. In the kinetic model, the adsorptions of Pb^{2+} and Cu^{2+} were higher than for the other heavy metal ions. The adsorption efficiencies of heavy metals in seawater did not decrease significantly in comparison with those in fresh water. In conclusion, red mud is a high-performance alternative compared to commercial zeolites, limestone, and oyster shell for the removal of heavy metal contaminants. Therefore, red mud can be considered as a capping-material alternative to remediate multi-heavy metal contaminated marine sediment.

Acknowledgments

This research was a part of the project titled "Development of Sustainable Remediation Technology for Marine Contaminated Sediments", funded by the Ministry of Oceans and Fisheries, Korea

References

1. Alloway BJ. Soil processes and the behaviour of metals. In: Alloway BJ, ed. Heavy metals in soils. New York: Halsted Press; 1990. p. 7-28.
2. Gray CW, Dunham SJ, Dennis PG, Zhao FJ, McGrath SP. Field evaluation of in situ remediation of a heavy metal contaminated soil using lime and red-mud. *Environ. Pollut.* 2006;142:530-539.
3. Lombi E, Zhao FJ, Zhang G, et al. In situ fixation of metals in soils using bauxite residue: chemical assessment. *Environ. Pollut.* 2002;118:435-443.
4. Basta NT, McGowen SL. Evaluation of chemical immobilization treatments for reducing heavy metal transport in a smelter-contaminated soil. *Environ. Pollut.* 2004;127:73-82.
5. Castaldi P, Santona L, Cozza C, et al. Thermal and spectroscopic studies of zeolites exchanged with metal cations. *J. Mol. Struct.* 2005;734:99-105.
6. Mule P, Melis P. Methods for remediation of metal-contaminated soils: preliminary results. *Commun. Soil Sci. Plant Anal.* 2000;31:3193-3204.
7. Bowman RS. Applications of surfactant-modified zeolites to environmental remediation. *Microporous Mesoporous Mater.* 2003;61:43-56.
8. Ouki SK, Kavannagh M. Performance of natural zeolites for the treatment of mixed metal-contaminated effluents. *Waste Manag. Res.* 1997;15:383-394.
9. Chvedova D, Ostap S, Le T. Surface properties of red mud particles from potentiometric titration. *Colloids Surf. A Physicochem. Eng. Asp.* 2001;182:131-141.
10. Liu Y, Naidu R, Ming H. Red mud as an amendment for pollutants in solid and liquid phases. *Geoderma* 2011;163:1-12.
11. Barnes D, Gould BW, Bliss PJ, Valentine HR. Water and wastewater engineering systems. London: Pitman Books; 1981.
12. Gazea B, Adam K, Kontopoulos A. A review of passive systems for the treatment of acid mine drainage. *Miner. Eng.* 1996;9:23-42.
13. Lopez E, Soto B, Arias M, Nunez A, Rubinos D, Barral MT. Adsorbent properties of red mud and its use for wastewater treatment. *Water Res.* 1998;32:1314-1322.
14. Castaldi P, Santona L, Melis P. Heavy metal immobilization by chemical amendments in a polluted soil and influence on white lupin growth. *Chemosphere* 2005;60:365-371.
15. Hsu TC. Experimental assessment of adsorption of Cu2+ and Ni2+ from aqueous solution by oyster shell powder. *J. Hazard. Mater.* 2009;171:995-1000.
16. Ho YS, McKay G. The sorption of lead(II) ions on peat. *Water Res.* 1999;33:578-584.
17. Ho YS, McKay G. Pseudo-second order model for sorption processes. *Process Biochem.* 1999;34:451-465.
18. Bertocchi AF, Ghiani M, Peretti R, Zucca A. Red mud and fly ash for remediation of mine sites contaminated with As, Cd, Cu, Pb and Zn. *J. Hazard. Mater.* 2006;134:112-9.
19. Ruan HD, Frost RL, Kloprogge JT. The behavior of hydroxyl units of synthetic goethite and its dehydroxylated product hematite. *Spectrochim. Acta A Mol. Biomol. Spectrosc.* 2001;57:2575-2586.
20. Castaldi P, Silvetti M, Santona L, Enzo S, Melis P. XRD, FTIR, and thermal analysis of bauxite ore-processing waste (red mud) exchanged with heavy metals. *Clays Clay Miner.* 2008;56:461-469.
21. Tongamp W, Kano J, Zhang Q, Saito F. Simultaneous treatment of PVC and oyster-shell wastes by mechanochemical means. *Waste Manage.* 2008;28:484-488.
22. Liu Y, Lin C, Wu Y. Characterization of red mud derived from a combined Bayer Process and bauxite calcination method. *J. Hazard. Mater.* 2007;146:255-261.
23. Lee CW, Kwon HB, Jeon HP, Koopman B. A new recycling material for removing phosphorus from water. *J. Clean. Prod.* 2009;17:683-687.
24. Hui KS, Chao CY, Kot SC. Removal of mixed heavy metal ions in wastewater by zeolite 4A and residual products from recycled coal fly ash. *J. Hazard. Mater.* 2005;127:89-101.
25. Lee M, Paik IS, Kim I, Kang H, Lee S. Remediation of heavy metal contaminated groundwater originated from abandoned mine using lime and calcium carbonate. *J. Hazard. Mater.* 2007;144:208-214.
26. Srivastava P, Singh B, Angove M. Competitive adsorption behavior of heavy metals on kaolinite. *J. Colloid Interface Sci.* 2005;290:28-38.
27. Soner Altundogan H, Altundogan S, Tumen F, Bildik M. Arsenic removal from aqueous solutions by adsorption on red mud. *Waste Manag.* 2000;20:761-767.
28. Panayotova M, Velikov B. Influence of zeolite transformation in a homoionic form on the removal of some heavy metal ions from wastewater. *J. Environ. Sci. Health A Tox. Hazard. Subst. Environ. Eng.* 2003;38:545-554.
29. Panayotova M, Velikov B. Kinetics of heavy metal ions removal by use of natural zeolite. *J. Environ. Sci. Health A Tox. Hazard. Subst. Environ. Eng.* 2002;37:139-147.
30. Chen GZ, Fray DJ. Cathodic refining in molten salts: removal of oxygen, sulfur and selenium from static and flowing mol-

ten copper. *J. Appl. Electrochem*. 2001;31:155-164.
31. Southichak B, Nakano K, Nomura M, Chiba N, Nishimura O. Pb(II) biosorption on reed biosorbent derived from wetland: effect of pretreatment on functional groups. *Water Sci. Technol*. 2006;54:133-141.
32. Wu FC, Tseng RL, Juang RS. Kinetic modeling of liquid-phase adsorption of reactive dyes and metal ions on chitosan. *Water Res*. 2001;35:613-618.
33. Hu J, Chen C, Zhu X, Wang X. Removal of chromium from aqueous solution by using oxidized multiwalled carbon nanotubes. *J. Hazard. Mater*. 2009;162:1542-1550.
34. Wang S, Terdkiatburana T, Tade MO. Adsorption of Cu(II), Pb(II) and humic acid on natural zeolite tuff in single and binary systems. *Sep. Purif. Technol*. 2008;62:64-70.
35. Snars K, Gilkes RJ. Evaluation of bauxite residues (red muds) of different origins for environmental applications. *Appl. Clay Sci*. 2009;46:13-20.
36. Hatje V, Payne TE, Hill DM, McOrist G, Birch GF, Szymczak R. Kinetics of trace element uptake and release by particles in estuarine waters: effects of pH, salinity, and particle loading. *Environ. Int*. 2003;29:619-629.
37. Misak NZ, Ghoneimy HF, Morcos TN. Adsorption of Co2+ and Zn2+ ions on hydrous Fe(III), Sn(IV), and Fe(III)/Sn(IV) oxides: II. Thermal behavior of loaded oxides, isotopic exchange equilibria, and percentage adsorption-pH curves. *J. Colloid Interface Sci*. 1996;184:31-43.